Revista de Teledetección. 2004. 22: 19-23.

Comparison of three atmospheric data in a solar spectrum atmospheric correction system

L. Martínez, V. Palà and R. Arbiol
lmartinez@icc.es

Remote Sensing Department, Institut Cartogràfic de Catalunya (ICC)
Parc de Montjuïc, s/n, 08037 Barcelona (Spain)

RESUMEN

En este trabajo se presenta un sistema de corrección atmosférica en dos pasos para espectro solar, y se compara el resultado de emplear datos atmosféricos del modelo MASS (Mesoscale Atmospheric SImulation System), radiosondeos y perfiles estándar. El primer paso del sistema es un modelo semiempírico que incluye transferencia radiatia a partir del código 6S (Second Simulation of the Satellite Signal in the Solar Spectrum). El segundo paso es un modelo empírico basado en zonas seudo-invariantes localizadas mediante una transformación TC (Tasselled Cap). Las correcciones atmosféricas se realizaron en una serie multitemporal pancromática Landsat 7 de Barcelona. Tras el primer paso el mejor resultado se logró con datos atmosféricos estándar. Tras el segundo paso se obtuvieron resultados similares con los tres tipos de datos.

PALABRAS CLAVE: corrección atmosférica, 6S, TC, radiosondeo, MASS, Landsat 7.

ABSTRACT

In this paper, a two-step atmospheric correction system for solar spectrum is presented. In addition, the results when using MASS (Mesoscale Atmospheric Simulation System) forecasted data, radiosoundings and standard profiles are compared. The first step of the system is a semi-empirical model and it includes radiative transfer simulation from the 6S (Second Simulation of the Satellite Signal in the Solar Spectru,) code. The second step is an empirical model based on pseudo-invariant areas located by means of of a TC (Tasselled Cap) transformation. The atmospheric corrections were performed on a multitemporal series of Landsat 7 panchromatic images from Barcelona. After the first step, the best result was achieved using standard atmospheric data. After the second step, similar results were obtained with all three kinds of data.

KEY WORDS: atmospheric correction, 6S, TC, radio-sounding, MASS, Lanadsat 7.

INTRODUCTION

Solar-spectrum passive remote sensing sensors measure mainly the radiance reflected by the atmosphere-ground system, since thermal emissions are insignificant in the solar-spectrum wavelength region. These images contain several kinds of geometric and radiometric distortions. Radiometric distortions should be corrected in order to obtain accurate physical measurements, to develop studies based on multitemporal series of images, or to compare images acquired with different sensors.

Radiance measured by a sensor depends on the illumination geometry and on reflectance characteristics of the observed surface. However, two atmospheric radiative processes disturb this measurement: gas absorption and both Rayleigh and Mie scattering. Absorption is an inelastic energetic process and is highly wavelength-dependent. On the other hand, scattering is an elastic interaction process with a smooth wavelength dependency that only changes the electromagnetic wave propagation pathway. Rayleigh scattering is caused by gaseous particles, while Mie scattering is due to aerosols. Scattering causes the so-called adjacent effect: a wrong measurement effect caused by radiation incoming from the surrounding area where the observed surfaced is located. Therefore, each radiance measurement is contaminated in an amount that depends on the radiance of its neighbouring pixels.

Atmospheric-effect corrected remote sensing measurements are routinely obtained at “Institut Cartogràfic de Catalunya” (ICC) with a self-developed solar spectrum atmospheric correction system. It consists of a two-step system that links together a semi-empirical method based on a physical model, followed by an empirical method based on normalizing the radiometry of pseudo-invariant areas. The system is modular and it is suitable for any sensor or platform. The semi-empirical step allows the incorporation of synchronous ancillary atmospheric data during the radiative transfer simulation process, in order to individually obtain absolute radiance measurements on every image. Later, the empirical step refines the multitemporal series of remote sensing data.

Several meteorological measurements or forecasted data are available from meteorological services such as the "Servei Meteorològic de Catalunya" (SMC). Radio-soundings are widely performed, while high precision numerical forecast simulations are less frequently performed, but also available. On the other hand, standard atmospheric data can be used if synchronous ancillary data are not available.

The objective of this work is to compare the results of atmospheric correction with the two-step atmospheric correction system from ICC on a pancromatic Landsat 7 multitemporal set of images when using those three types of atmospheric data.

SYSTEM METHODOLOGY

A. Semi-empirical step

The semi-empirical step is applied to radiance measured by the sensor or Top Of Atmosphere (TOA) radiance; as a result, the corrected reflectance or Bottom Of Atmosphere (BOA) reflectance is obtained.

Equivalent extraterrestrial reflectance or TOA reflectance, ρ^* can be expressed, in terms of measured radiance L^* as

$$\rho^* = \frac{\pi \, . \, L^*}{\mu_s \, . \, E_s} \quad (1)$$

where E_s is the extraterrestrial solar irradiance and μ_s is the zenital solar angle cosine.

Taking into account the interaction phenomena described in Staenz & Williams (1997), it is possible to express the radiance at the sensor, when observing a horizontal surface, as

$$L^* = A \frac{P_c}{(1 - <\rho_e> S)} + B \frac{<\rho_e>}{(1 - <\rho_e> S)} + L_a \quad (2)$$

were ρ_c is the corrected reflectance of the surface, $<\rho_e>$ is the corrected reflectance of the neighbourhood, S is the atmospheric albedo, L_a is the radiance backscattered to the sensor, and A and B are coefficients related to the direct and diffuse radiance.

Therefore, the corrected reflectance ρ_c, or BOA reflectance, for the observed surface is

$$p_c = \frac{(L^* - L_a)\,(1 - <\rho_e> S) - <\rho_e> B}{A} \quad (3)$$

The parameters A, B, S and L_a characterize both observation and illumination geometries and the atmospheric conditions when the image was obtained. Their values depend neither on the observed surface reflectance, nor on the neighbourhood's. Hence, they are calculated from the magnitudes L_g, which is the radiance entering the sensor from the observed surface, and L_p which is the radiance entering the sensor from the neighbourhood of the observed surface and backscattered by the atmosphere towards the sensor. If the surface has a uniform reflectance, those magnitudes will be

$$L_c = A \frac{P_c}{1 - S\rho_e} \qquad L_p = B \frac{P_c}{1 - S\rho_e} + L_a \quad (4)$$

Both L_g and L_p can be obtained by means of radiative transfer codes working on direct form. The values of A, B, S and L_a are directly obtained by solving the corresponding equations systems. The radiative transfer simulations are performed using the synchronous atmospheric data available.

The neighbourhood corrected reflectance $<\rho_e>$ will be obtained using in equation 2 the whole neighbourhood as if it were a hypothetic single pixel located in a uniform reflectance environment, so in that expression $<\rho_e>$ will be equal to ρ_c. Also, its radiometry L^* will be calculated using the whole neighbourhood's pixels radiometry. From these hypotheses, the value of $<\rho_e>$ will be

$$<\rho_c> = \frac{L^* - L_a}{A + B + S\,(L^* - L_a)} \quad (5)$$

B. Empirical step

A set of multitemporal images that have been previously corrected with the proposed semi-empirical method, is suitable for an additional correction with a pseudo-invariant areas normalization method. The illumination and the atmospheric conditions throughout the image have been some of the drawbacks for a systematic and broad use of these statistical methodologies. Nevertheless, with the proposed two-step methodology, statistical methodologies can be applied regardless of the original illumination and atmospheric condition when the image was acquired.

That sort of procedure generates more radiometrically homogeneous temporal series that also are compensated for atmospheric characterization deviations, sensor calibration drift, etc (Caselles & López, 1989). Finally, BOA reflectance for those pseudo-invariant areas is used to calculate bias and gain coefficients for the corrected reflectance along the whole set.

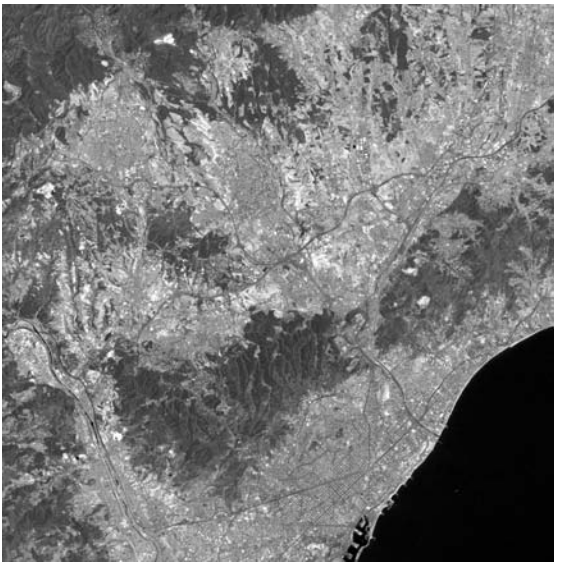

Figura 1. Subscene of Barcelona metropolitan area analysed.

EXPERIMENTAL RESULTS

The Atmospheric Correction System has been adapted in order to perform atmospheric correction on a series of six panchromatic images, whose main characteristics are depicted in Table 1, acquired by the Enhanced Thematic Mapper Plus (ETM+) sensor on board of Landsat 7 platform. In this work, the analysed subscene is located in the Barcelona metropolitan area and can be seen in Figure 1. The image set is geometrically corrected by means of a blundle adjustment using the geometric model described in Palà & Pons (1995). The geocoded set was rectified on a 15m spaced mesh using a nearest neighbour interpolation technique.

Acquisition Dates	Acquisition Time (UTC	Solar Elevation (deg)
23-jul-1999	10:23	60.9º
09-set-1999	10:23	49.2º
30-dec-1999	10:23	22.0º
03-mar-2000	10:23	36.7º
07-jun-2000	10:22	64.0º
11-set-2000	10:21	48.1º

Tabla 1. Landsat 7 ETM+ pan imagery series information.

Radiative transfer simulations for the application of the physical model were done using the Second Simulation of the Satellite Signal in the Solar Spectrum (6S) code (Vermote *et al.*, 1997). The available ancillary meteorological data were:

• World Wide Standard Atmosphere from 6S.

• MASS (Mesoscale Atmospheric Simulation System) (Codina *et al.*, 1997). It is a usual tool used at SMC for accurate weather forecasting. On purpose, calculations were performed to obtain data that is almost synchronous (09:00 UTC) with the images. Grid spacing was 15 km and temperature, dew point and geopotential height was provided between 1000 and 100 hPa, at 25 hPa steps.

• Radio-sounding profiles are widely used measurements of the physical state of the atmosphere. It is routinely performed at SMC twice a day, at 24:00 and 12:00 UTC, from Barcelona. The last one was chosen since it was the closest to the imagery acquisition time.

Besides, a standard climatologic aerosols model, and a Digital Elevation Model with the same resolution as the imagery, were introduced in the simulator.

Pseudo-invariant areas were chosen by means of a TC (Tasselled Cap) transformation for ETM+ as explained in Huang *et al.* (2002). Nine pseudo-invariant areas were found using that methodology and an additional area over the sea was included. The ten areas used to perform lineal regressions can be seen in Figure 2. Those areas had low values for the second TC component, but a wide range of values for the first component of the TC transformation. As can be seen in Figure 3, radiometric values for all those areas were used to perform lineal regressions between each image and the first component of the series. The r^2 values were over 0.98 in all the cases. These results indicate a good performance of the invariant areas selection algorithm, in spite of the shadowing differences over the time present in an urban environment (Palà & Arbiol, 2002).

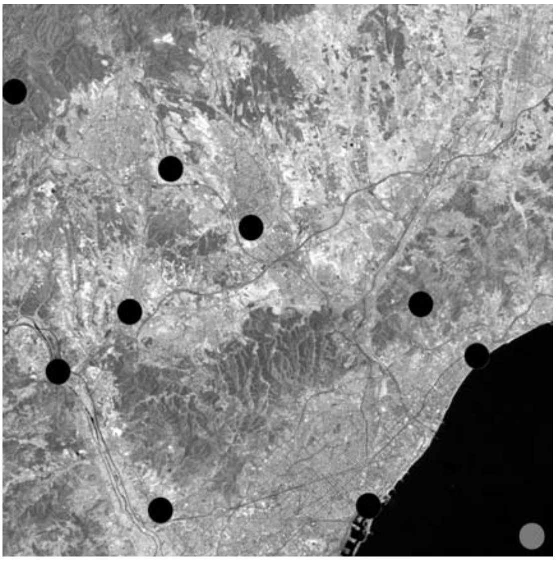

***Figura 2.** Pseudo-invariant and sea areas used to perform lineal regressions.

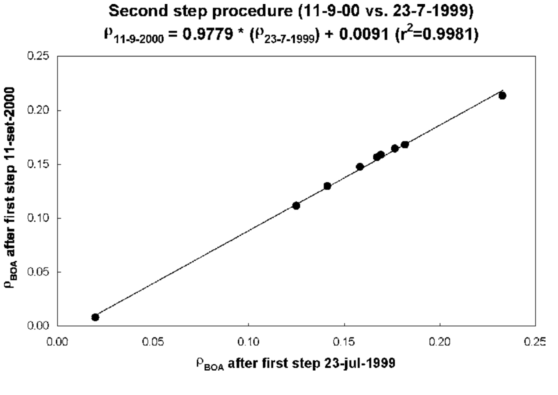

Figura 3. Example of the second step procedure.

As it is detailed in Table 2, atmospheric uncorrected reflectance (TOA reflectance) from the areas established as pseudo-invariant has a RMS of 0.012 for the whole series. Atmospheric corrected reflectance (BOA reflectance) obtained using the semi-empirical method and the Standard Atmosphere had a RMS value of 0.010 for the whole series. RMS for both the MASS and Radio-sounding data was 0.011. That value is slightly better than the uncorrected one, but does not improve the results obtained when using the standard data. When the empirical method was applied on data already corrected with the semi-empirical method, corrected data reduced their RMS to 0.006, which is half the value before applying the Atmospheric Correction System.

Correction Method Applied	RMS of Reflectance Series
Uncorrected	0.012
Semi-empirical step (Standard Data)	0.010
Semi-empirical step (MASS Data)	0.011
Semi-empirical step (Radio-sounding Data)	0.011
Semi-empirical step + Empirical step	0.06

Tabla 2. RMS of reflectance series before and after atmospheric corrections.

The obtained reduction of RMS with the first step is not very important even when non-standard data are incorporated, but it must be noted that this procedure allows the use of the normalization processes regardless of geometric and atmospheric conditions.

CONCLUSIONS

In this work a comparison between standard, radiosounded and forecasted atmospheric data in a solar spectrum atmospheric correction system has been done. The system has been adapted to perform atmospheric correction on a series of six Landsat 7 ETM+ panchromatic images. Nine pseudo-invariant areas were found by means of a TC transformation. After the correction is performed with a semi-empirical method, the reflectance on pseudo-invariant areas showed the best results using atmospheric standard data, but good results were also obtained when MASS and Radio-sounding data were used. Moreover, empirical correction halved the initial RMS.

Todas las figuras precedidas de asterisco se incluyen en el cuadernillo anexo de color

ACKNOWLEDGMENTS

The authors are very grateful to Eliseu Vilaclara Ribas and Abdelmalik Sairouni from SMC for MASS forecasted data and atmospheric radio-sounding data delivered. We also are grateful to all the reviewers for their helpful suggestions.

BIBLIOGRAPHY

CASELLES, V. & LÓPEZ, M.J. 1989. An alternative simple approach to estimate atmospheric correction in multitemporal studies, *IJRS*. 10: 1127-1134.

CODINA, B., ARAN, M., YOUNG, S. & REDAÑO, A. 1997. Prediction of a Mesoescale Convective System over Catalonia (Northeastern Spain) with a Nested Numerical Model. *Meteor. Atmos. Phys*. 62: 9-22.

HUANG, C., WYLIE, B., HOMER, C., YANG, L. & ZYLSTRA, G. 2002. Derivation of a Tasseled cap transformation based on Landsat 7 at-satellite reflectance. *IJRS*. 23 (8): 1741-1748.

PALÀ, V. & ARBIOL, R. 2002. True orthoimage generation in urban areas. *Proceedings of 3rd International Symposium Remote Sensing of Urban Areas*. Vol 1, pp. 309-314. Estambul.

PALÀ, V. & PONS, X. 1995. Incorporation of relief in polynomial-based geometric correcctions. *PE&RS*. 61: 935-944.

STAENZ, K. & WILLIAMS, D.J. 1997. Retrieval of Surface Reflectance from Hiperespectral Data Using a Look-up Table Approach. *CJRS*. 23 (4): 354-368.

VERMOTE, E., TANRÉ, D., DEUZÉ, J.L., HERMAN, M. & MORCRETTE, J.J. 1997. Second simulation of the satellite signal in the solar spectrum, 6S: an overview. *IEEE TGRS*. 35: 675-686.

NOTICIAS

La revista de Teledetección insertará figuras EN COLOR, acompañando los textos de los artículos seleccionados.

Mediante esta decisión, se vuelve a recuperar uno de los objetivos iniciales de la revista. Parecía una necesidad obvia incluir los resultados gráficos en color para alcanzar mayor calidad de este instrumento de comunicación entre los miembros de la comunidad científica española que trabaja en Teledetección.

Por tanto, desde estas páginas se anima de nuevo a todos aquellos profesionales involucrados en estudios científicos o técnicos de Teledetección a que envíen sus trabajos a la revista, considerando esta nueva posibilidad.

Seguimos trabajando en la mejora de calidad de la revista. Serán bienvenidas todas aquellas sugerencias que permitan alcanzar ese objetivo.